Environ Earth Sci (2016)75:643
DOI 10.1007/s12665-016-5463-2

ORIGINAL ARTICLE

Assessment of groundwater contamination around active dumpsite in Ibadan southwestern Nigeria using integrated electrical resistivity and hydrochemical methods

S. A. Ganiyu[1] · B. S. Badmus[1] · M. A. Oladunjoye[2] · A. P. Aizebeokhai[3] · V. C. Ozebo[4] · O. A. Idowu[5] · O. T. Olurin[1]

Received: 19 December 2014 / Accepted: 12 February 2016

Abstract Investigation of groundwater contamination due to leachate migration in a solid waste disposal site was done using both geophysical and hydrochemical methods. The main goals were to delineate groundwater contamination due to leachate percolation and thus assessment of quality of groundwater from nearby hand-dug wells bordering the dumpsite for drinking purpose. A total of ten resistivity traverses were acquired within and outside the dumpsite using Wenner configuration with constant electrode separation ranging from 5 to 25 m. The 2D resistivity data were processed and inverted using RES2DINV and RES3DINV softwares, respectively. Geochemical assessment of groundwater samples were carried out according to APHA standards while hydrochemical facies of the sampled groundwater was evaluated using Piper Trilinear software. The inverse resistivity models of the subsurface from 2D and 3D imaging revealed low resistivity value less than 10 Ω m suspected to be leachate while 3D inverse sections allowed delineation of leachate, weathered layer, bedrock and seepage path from the dumpsite. The extent of migration was more pronounced in the southern part of the dumpsite, hence possible contamination of shallow groundwater system as dumpsite ages. The results of physico-chemical analyses showed the groundwater samples to be within the limits of WHO/NSDWQ for drinking purpose. However, higher values of concentrations of most analyzed parameters were noticed in well 1 due to its nearness to dumpsite and well 10 due to agricultural activities, respectively. Interpretation of Piper diagram showed $CaHCO_3$ to be dominant facie in the area while alkaline earth metals (Ca^{2+}, Mg^{2+}) and weak acids (HCO_3^-, CO_3^-) are dominant cations and anions during both climatic seasons. Groundwater in the study area is of hard, fresh and alkaline in nature.

Keywords Solid waste · Dumpsite · Resistivity · Leachate · Hydrochemical facies · Contamination

Introduction

Industrial development and uncontrolled increase of rural–urban migration have resulted iin increase in production rate of different types of wastes ranging from municipal to industrial which have adverse effects on human health via groundwater quality (Ramakrishnaiah et al. 2009). According to Rizwan and Gurdeep (2010), groundwater quality depends on the quality of recharged water, quantity and quality of generated waste, sewage treatment and subsurface geochemical processes. Groundwater contamination is a challenging phenomenon in the country since most of the cities in the country face solid waste management problems such as poor waste collection, inadequate waste disposal equipment, indiscriminate dumping of wastes on streets and canals, siting of waste disposal site

✉ S. A. Ganiyu
adekunsa@yahoo.com

[1] Department of Physics, Federal University of Agriculture, Abeokuta, Ogun State, Nigeria

[2] Department of Geology, University of Ibadan, Ibadan, Oyo State, Nigeria

[3] Department of Physics, Covenant University, Ota, Ogun State, Nigeria

[4] Department of Physics, University of Lagos, Akoka, Lagos State, Nigeria

[5] Department of Water Resources and Agrometeorology, Federal University of Agriculture Abeokuta, Abeokuta, Ogun, Nigeria

Published online: 11 April 2016

within residential areas without regard to local geology and hydrogeology of the area. All these factors contribute to the contamination of the nearby groundwater resources. Urban waste materials (municipal and industrial) are usually disposed off inadequately in waste dumpsite thus posing a high risk to the underground water resources, environmental pollution and community health (Soupios et al. 2006). Open dumpsite near the residential area can have adverse effect on nearby water sources if the leachate emanated from decomposed solid waste infiltrates and pollutes the water table. High concentration of ionic constituents of leachate are usually obtained from municipal waste disposal site and can inflict health risk to both population and natural environment (Andrea et al. 2012).

The electrical resistivity technique has been widely used in environmental geotechnical investigation on the field (Mondelli et al. 2010; Ustra et al. 2012). Electrical resistivity method is also useful in the evaluation of topsoil thickness, competence and corrosivity to determine the suitability of soil for construction and foundation design purposes (Bayowa and Olayiwola 2015). Resistivity measurement can be affected by seasonality of moisture content, soil porosity, degree of saturation, temperature and salinity of the percolation fluid (Yamasaki et al. 2013). Johansson et al. (2011) also studied the influence of the soil gas phase on electrical resistivity by considering both spatial and temporal variations of soil gas flow via landfill. Munoz-Castelblanco et al. (2011) show that the electrical resistivity of Loess soil can be divided into two regions based on soil micropores. These are inter-aggregate pores in which the water phase is continuous while the second regime corresponds to the intra-aggregate pores where the water phase is disconnected as a result of the presence of empty pore space between the aggregates. Hydraulic conductivity is defined as the meters per day of water seeping into the soil under the pull of gravity or under a unit of hydraulic gradient (Kirkham 2005). Knowledge of hydraulic conductivity is very important in solving various environmental problems as it is one of the most important sol properties for the determination of infiltration rate, control of irrigation and drainage processes and other hydrological processes (Gulser and Candemir 2008). It is also useful in controlling water infiltration, leaching of pesticides from cultivated land, surface run-off and migration of pollutants from contaminated sites to the nearby groundwater resources (Bagarello and Sgroi 2007).

Electrical resistivity of permafrost table depends on the temperature, pore water salinity, porosity, unfrozen water and ice contents, cryostructure, material types and electrode array geometry (Fortier et al. 1994). Permafrost issues resolvable by geophysical techniques include the assessment of temporal variations in subsurface geophysical properties due to permafrost cooling, warming, aggradation and degradation through geophysical monitoring (Kneisel et al. 2008). Yu et al. (2003) carried out permafrost investigation using various geophysical methods while 2D electrical resistivity imaging was used to investigate structure of patterned ground as well as to interpret the relationships between ground structure and the geometry of the permafrost table (Kasprzak 2015). Electrical resistivity has been employed over the years to characterize aquifer in different geologic environments, delineation of subsurface lithology and mapping of possible fractured assisted aquifer system (Adepelumi et al. 2008; Ayolabi et al. 2009; Lateef 2012).

Several research activities on groundwater contamination arising from nearby solid waste disposal sites based on geochemical analyses have been carried out (Assmuth and Strandberg 1993; Matias et al. 1994; Kayabali et al. 1998; Ikem et al. 2002; Tijani et al. 2002; Armah et al. 2012; Afolayan et al. 2012; Badejo et al. 2013). Most of these studies aimed at defining the spatial extent of groundwater contamination based on the result of chemical analyses.

Leachate plume generated at a waste disposal site contains high ion concentrations and thus have low resistivity values. This makes an electrical imaging technique a reliable tool for mapping contamination plumes generated from solid waste dumpsite. Amongst other geophysical technique, electrical method is the most preferred for dumpsite investigation as it can delineate contaminated zones of groundwater effectively due to conductive nature of most contaminants (Mazac et al. 1987; Atekwana et al. 2000; Karlik and Kaya 2001).

Electrical resistivity method is versatile, fast, cost effective and a non-destructive geophysical technique for mapping the shallow subsurface anomaly. Electrical resistivity imaging has no adverse impacts to the environment and serves as a good method for delineating the relatively rapid variations in the subsurface during environmental remediation (Kumar 2012).

Most published studies have detailed the use of 2D electrical resistivity tomography for dumpsite investigation (Soupios et al. 2006; Adepelumi et al. 2008; Abdullahi et al. 2011; Jegede et al.2011; Oladunjoye et al. 2011; Iyoha et al. 2013; Yalo et al. 2014) as well as tracing of subsurface oil pollution leakage (Win et al. 2011; Metwaly et al. 2012). The integrated use of hydrochemical and geophysical methods is often recommended (Benson et al. 1983; Matias et al. 1994; Kayabali et al. 1998; Ariyo and Enikanoselu 2007).

A combination of hydrochemical and geophysical methods was used in a groundwater contamination study around Ajakanga dumpsite located in southwestern part of Nigeria. By combining the results of geophysical and hydrogeochemical analyses from existing hand-dug wells around the dumpsite, a detailed empirical information about the dumpsite as well as better understanding of

spatial extent of leachate plume migration, hydrogeochemical constituents of groundwater and its suitability for domestic purpose can be obtained. This work is aimed to examine the impact of solid waste disposal site on groundwater quality through the identification and delineation of the extent of contaminated leachate plume migration below the surface, mapping the presence of subsurface structures below the ground surface that could act as pathways for the flow of the contaminant. Finally to examine the health implication of generated leachate on nearby groundwater through hydrochemical and microbial analyses so as to assess the level of contamination of groundwater from hand-dug wells within the vicinity of the dumpsite.

Site description and geological setting

Ibadan is located approximately within the square of latitude 7°20′ to 7°40′ North of the equator and longitude 3°35′ to 4°10′ East of the Greenwich meridian. There are three major rivers draining the city, these are Ogunpa, Ogbere and Ona rivers with many tributaries (Fig. 1). Ajakanga open solid waste site in Ibadan is situated over 10 ha of land along Challenge road and was opened since 1998 and still active till date. The general overview of the dumpsite is shown in Fig. 2. The study area lies within longitudes 3°50′187″E and 3°50′696″E and latitudes 7°18′021″N and 7°18′997″N. It is owned and maintained by Oyo State Waste Management Authority. In Ibadan city, solid waste generation is on the increase. The city currently generates about 1,618,293 kg of solid waste daily with about 10 % of this evacuated by the Oyo State Waste Management Authority, the local government and the private refuse contractors while the remaining 90 % is left to households, commercial and industrial generators to dispose off in form of burning, dumping on streets, drain etc. (CPE 2010). The study area falls within the humid and subhumid tropical climate of southwestern Nigeria with a mean annual rainfall of about 1270 mm mean annual potential evaporation of 1199 mm and a mean maximum temperature of 32 °C (Akintola 1986). The soil type of the study area belongs to Orthic Luvisols (FAO 2015). The water retention capacity values of the experimental soil samples at different points within the dumpsite ranged from 10.4 to 38.4 % with a mean value of 37.3 % using the pressure plate apparatus following Dane and Hopmans (2002) procedures.

The study area falls within the basement complex terrain of southwestern Nigeria. The basement complex rocks

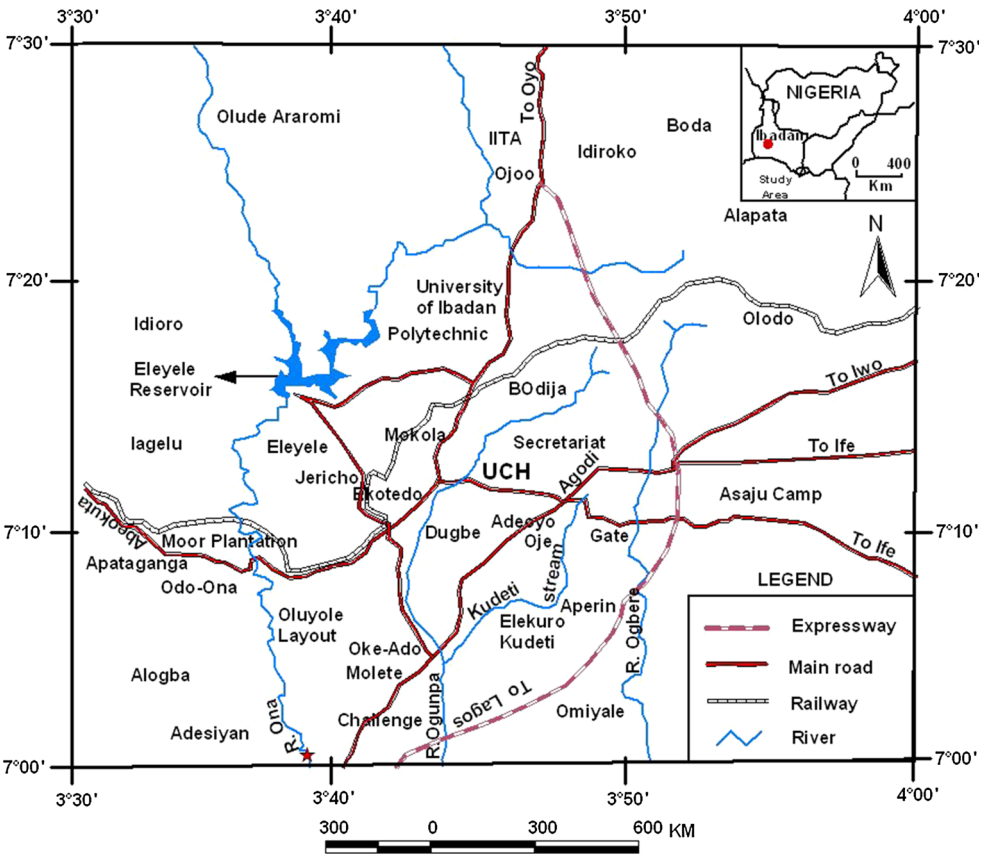

Fig. 1 Map of Ibadan showing its different parts and the major rivers

Fig. 2 General overview of Ajakanga dumpsite (JPEG)

consist of crystalline igneous and metamorphic rocks, which form part of the African Crystalline shield with the rocks belonging to the youngest of the three major provinces of the West African Craton (Jones and Hockey 1964). These rocks occur either exposed or covered by shallow mantle of superficial deposits. They are loosely categorized into three main subdivisions namely the migmatite-gneiss complex; the schist belt and Pan-African (Ca 600 Ma) Older granite series (Elueze 2000). The generalized geological map of Ibadan is shown in Fig. 3. The basement complex rocks in their unaltered form are characterized by low porosity and permeability which determines the hydrogeological properties of the rocks depending on the texture and mineralogy of the rocks. The top soil has been disturbed in the study area and hence constitutes the waste dump and the leachate derived from its decomposition processing.

Methodology

2D electrical resistivity survey

Two-dimensional (2D) electrical resistivity survey was carried out within the dumpsite using Campus Tigre Terameter. Nine traverses were mapped out within the dumpsite and a control traverse at about 500 m away from the refuse dumpsite using the Wenner array configuration. Figure 4 shows the data acquisition map for resistivity survey. The electrode separation distance for each traverse ranged from $a = 5$–30 m with a station interval of 5 m. The Wenner electrode array has one current electrode (C_1) followed by two potential electrodes, (P_1 and P_2) and ends with second current electrode (C_2). The current and potential electrodes are maintained at a regular fixed distance from each other (starting at $a = 5$ m) and are progressively moved along the traverse line. The geometric factor (K) for the Wenner array equals $2\pi a$. Measurements commenced at one end of the traverse line with electrode spacing $a = 5$ m at electrode positions 1, 2, 3 and 4. Next, each electrode (C_1, P_1, P_2 and C_2) was shifted a distance of 5 m, the active electrode positions being 2, 3, 4 and 5. The procedure was continued to the end of the traverse line (as shown in Fig. 5). At each measurement, the resistivity meter displayed field resistance value and the corresponding root mean square (rms) error of the reading. The apparent resistivity of the subsurface can be computed using the formula $\rho_a = 2\pi aR$ where a is the electrode spacing distance and R is the field resistance value. The traverse length ranged from 70 to 200 m. Six out of nine traverses within the dumpsite were in N–S direction while the remaining three were in W–E direction. The orientation of control traverse was in N–S direction. The 2D inverse resistivity models of the subsurface was obtained from the

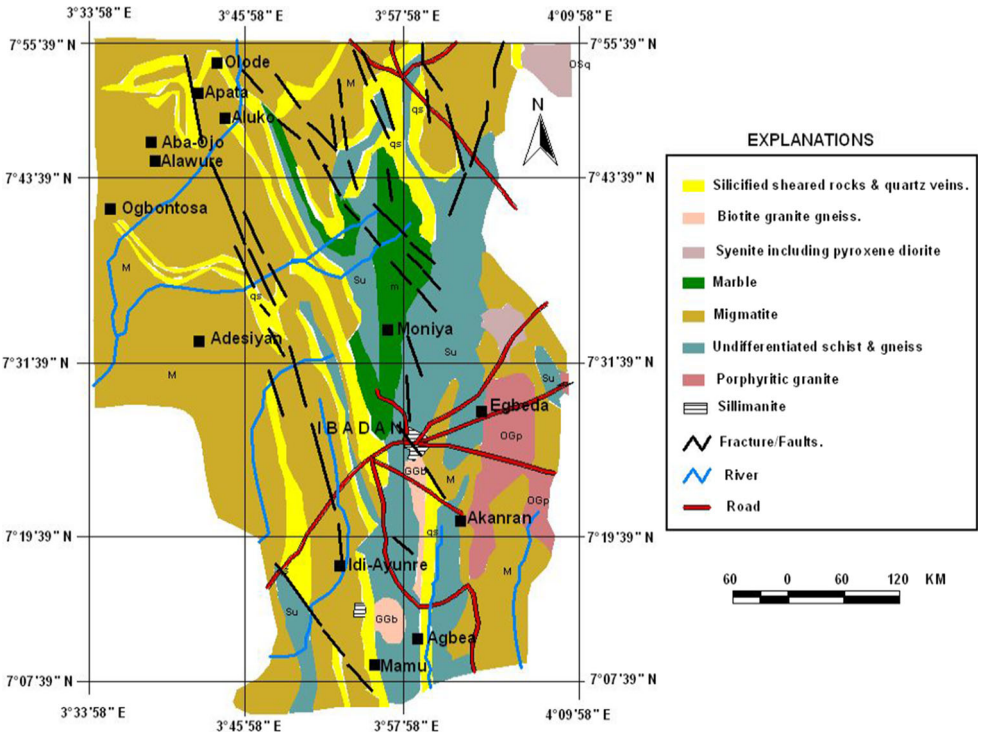

Fig. 3 Generalized geological map of Ibadan showing the study area (JPEG)

input resistivity data using inversion code of RES2DINV (Loke and Barker 1996; Loke 2000) while 3D inverse horizontal models of the subsurface was obtained from the inversion of 3D data set obtained from collated 2D resistivity data sets with the aid of RES3DINV computer program. These are inversion programs that automatically determines the 2D and 3D resistivity models of the subsurface from the input resistivity data using smoothness constrained least squares method (Sasaki 1992).

The resistivity measurement is based on the difference in resistivity values of the model blocks directing towards minimizing the difference between the calculated and the measured apparent resistivity values from the field. The accuracy of fit is expressed in terms of the RMS error (Loke and Barker 1996).

Chemical and microbial analyses of groundwater samples from hand-dug wells

Ten groundwater samples from hand-dug wells and stream were collected during dry and wet seasons at ten different locations around the dumpsite (Fig. 6). The distance of the hand-dug wells and stream to the dumpsite, depth of the well and static water level depth for both seasons were noted. Preservation of water samples and chemical analyses were carried out using standard procedures recommended by APHA (2005). Hydrogeochemical facies of analyzed groundwater samples was done with the aid of Piper Trilinear software. Microbial analyses of groundwater samples were done using total plate count method via media MacConkey Agar and Eosine methylene Blue Agar for detection of coliform bacteria and *E. coli* respectively. The analysed data can be used for the classification of water for various purposes and their percentage compliance with World Health Organization (WHO 2007) and Nigerian Standard for Drinking Water Quality (NSDWQ 2007) specified limits.

Results and discussion

Interpretation of 2D resistivity models

The inverse model sections of the subsurface and resistivity distribution derived from 2-D inversion are presented in Figs. 7, 8 and 9. As shown in Fig. 7a, the resistivity inverse model of traverse 1 shows continuous spread of leachate plume from horizontal distance of 8–82 m in the north–south direction with resistivity values below 10 Ω m, an indication of leachate plume accumulation up to 12 m depth below the surface and probably may have reach the water table due to weathered basement below the basin shaped leachate plume. The leachate migration on this traverse originates from the northern end of the traverse where it extends to the surface. Figure 7b shows model section for traverse 2 comprising of low resistivity anomalies with resistivity values below 10 Ω m, an indication of leachate at horizontal distance of 10–65 and

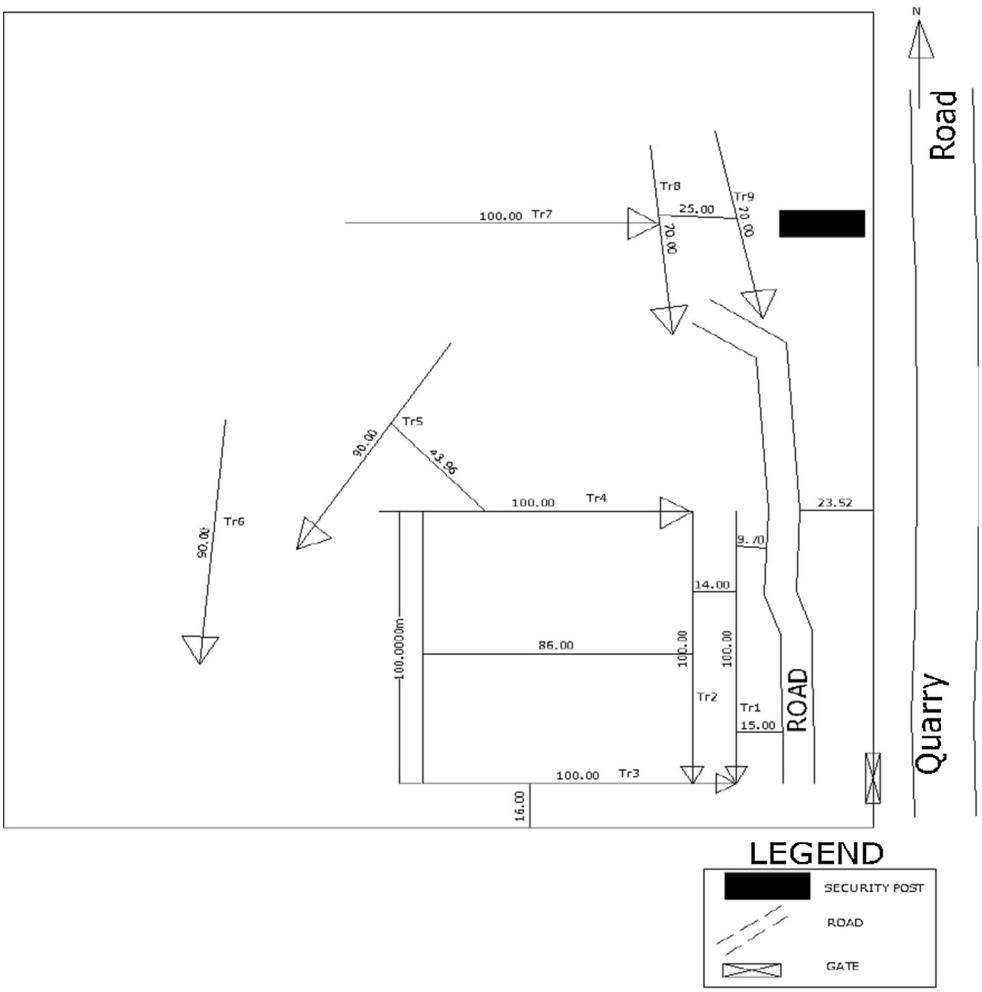

Fig. 4 Data acquisition map for electrical resistivity survey

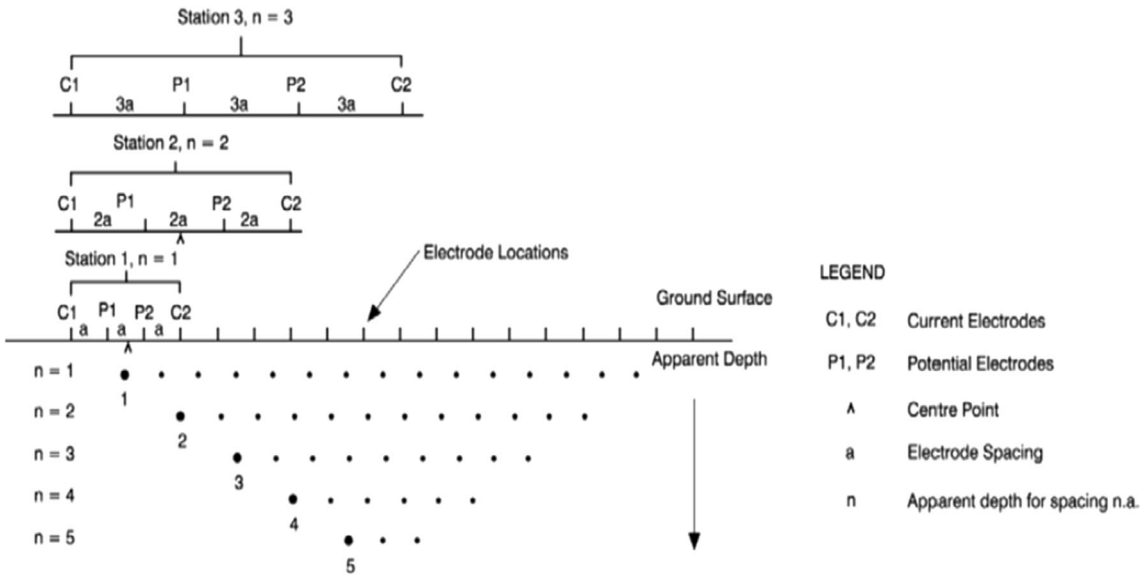

Fig. 5 Construction of a continuous resistivity profile using the Wenner array

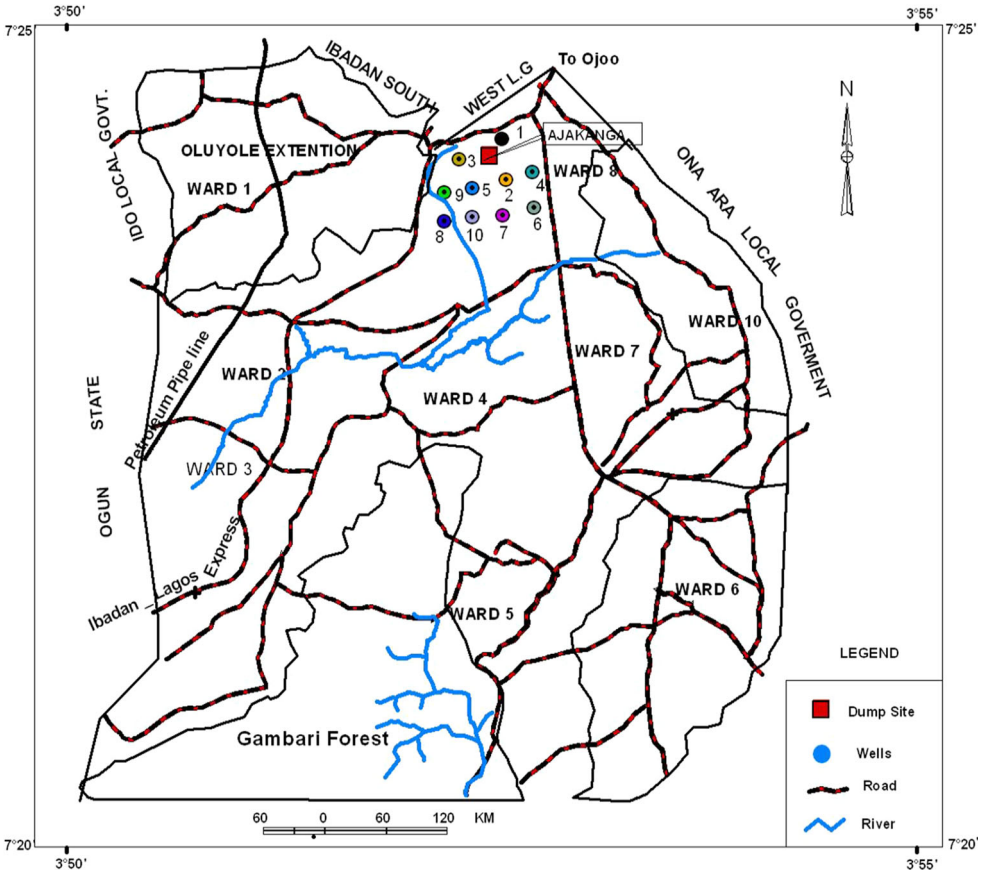

Fig. 6 Map of Ajakanga dumpsite and water sampling locations

68–92 m. The resistivity values throughout the traverse section were mostly less than 100 Ω m. Figure 7c shows inverse model section for traverse 3, wherein low resistivity anomalies below 10 Ω m, an indication of leachate plume migration occur at horizontal distances 10–35 and 41–85 m along the traverse. Following this plume is weathered zone at depth 12–15 m with resistivity values ranging from 17 to 132 Ω m indicating that the deeper layers are prone to groundwater contamination as dumpsite ages. Relatively high resistivity anomaly of resistivity values 17–79 Ω m to a depth of about 5 m occurs close to the surface suggesting presence of clayey sand mixed with non degradable waste material.

The inverse model resistivity sections of traverses 4, 5 and 6 are shown in Fig. 8a–c. As shown in Fig. 8a, two low-resistive anomalies were observed at positions 7–22 m and 27–45 m along the traverse with resistivity values between 5 and 8 Ω m. The low resistivity anomalies in the traverse show minor evidence of horizontal migration from western to eastern side and vertical migration up to about 4 m depth below the surface. This is followed by weathered basement rock of resistivity values between 12 and 95 Ω m. The model of traverse 5 shows an upper layer from surface to about 4 m having a low resistivity values below 10 Ω m, an evidence of leachate plume formation with nearly uniform lateral and depth extent. The low resistive anomaly of the upper layer indicates that the underlying layer has resistivity values ranging between 20 and 200 Ω m indicating weathered basement (Fig. 8b). In Fig. 8c, the 2D section shows low resistivity anomaly towards the southern part of the traverse at position 40–82 m with resistivity values between 10 and 20 Ω m, an indication of leachate plume occurring at a depth of about 4 m below the surface. The near surface low resistivity was not noticed between 7.5 and 40 m along the traverse. A relatively high resistivity anomalies with resistivity values between 40 and 338 Ω m of weathered materials were noticed at approximate depth 4–12 m. The lower part of the section shows an undulating bedrock at position 27 m in the northern part of the traverse to 62 m towards the southern part of the traverse with resistivity values between 688 and 1400 Ω m.

The inversion model of traverse 7 (Fig. 9a) showed two major low resistive anomalies and two minor ones. The major and minor resistive anomalies are situated at 18–47, 48–80 and 8–12 m and 85–92 m in the eastern part of the traverse respectively with resistivity values below 10 Ω m, an indication of leachate plume. Following the plume is an

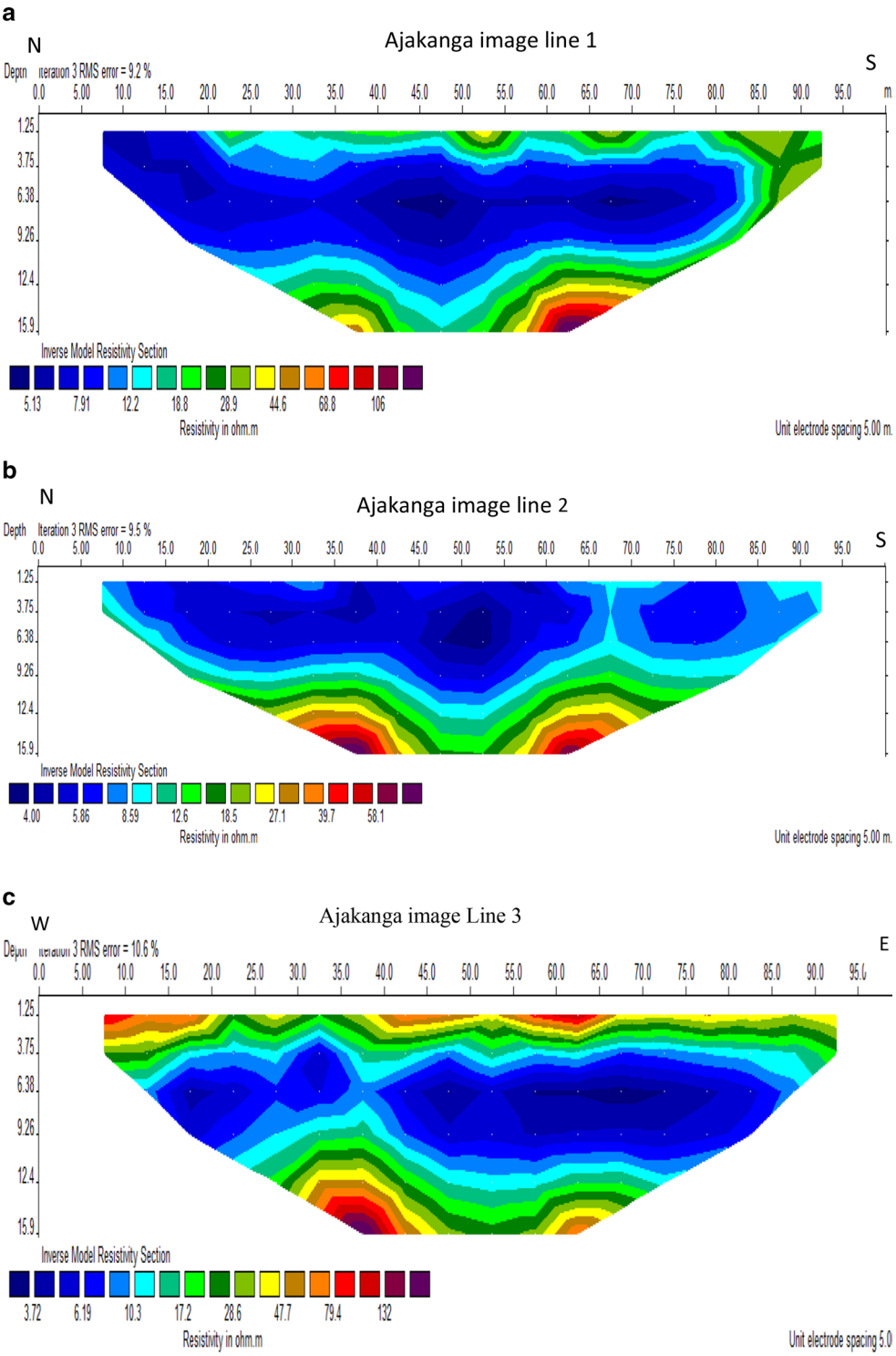

Fig. 7 2D inverse model resistivity sections for Ajakanga traverses 1, 2 and 3

underlying layer of resistivity values ranging between 40 and 338 Ω m indicating weathered materials. The model shows that the measurement encountered bedrock at horizontal position 30–72 m at approximate depth of 14–16 m.

Figure 9b shows inverse model section of traverse 8 in which at position 8–50 m towards the southern part of the traverse, there is presence of low resistive anomaly. The model shows the top 3 m of the regolith having low resistivity values between 11 and 20 Ω m, an indication that the top soil within this position range is made up of leachate accumulation. Generally for the traverse, the resistivity distributions are mostly less than 100 Ω m

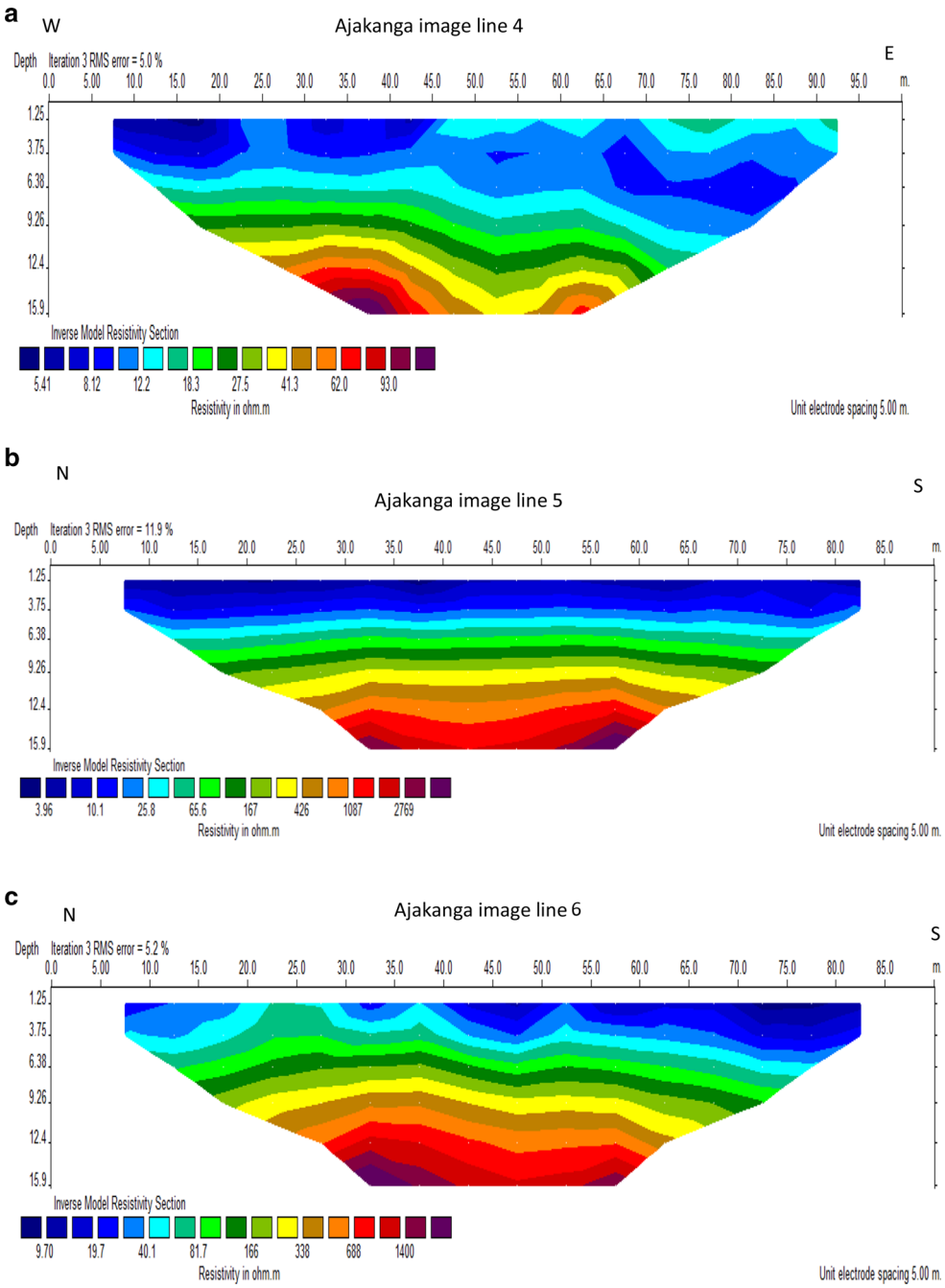

Fig. 8 2D inverse model resistivity sections for Ajakanga traverses 4, 5 and 6

throughout the traverse (Fig. 9b). In Fig. 9c, the inverse resistivity model section for traverse 9 showed low resistivity anomaly zone at position 7–42 m with resistivity values less than 20 Ω m occurring at approximately 4 m depth below the surface. This is an indication of leachate plume accumulation. The rest of the traverse towards the southern end of the traverse at horizontal distance of 45–64 m showed high resistivity anomaly between 29 and 43 Ω m protruding to the surface suggesting presence of clayey material mixed with non degradable wastes.

The inverse model section of control traverse is shown in Fig. 9d. High resistivity anomaly with resistivity values between 110 and 172 Ω m was noticed at northern part of the traverse at horizontal position 10–34 m while an isolated low resistive region of resistivity values between 29 and 45 Ω m, an indication of clay material was observed at position 38–47 m and 73–112 m along the traverse. This is an indication of no evidence of leachate accumulation on the control traverse as near surface resistivity values were higher than

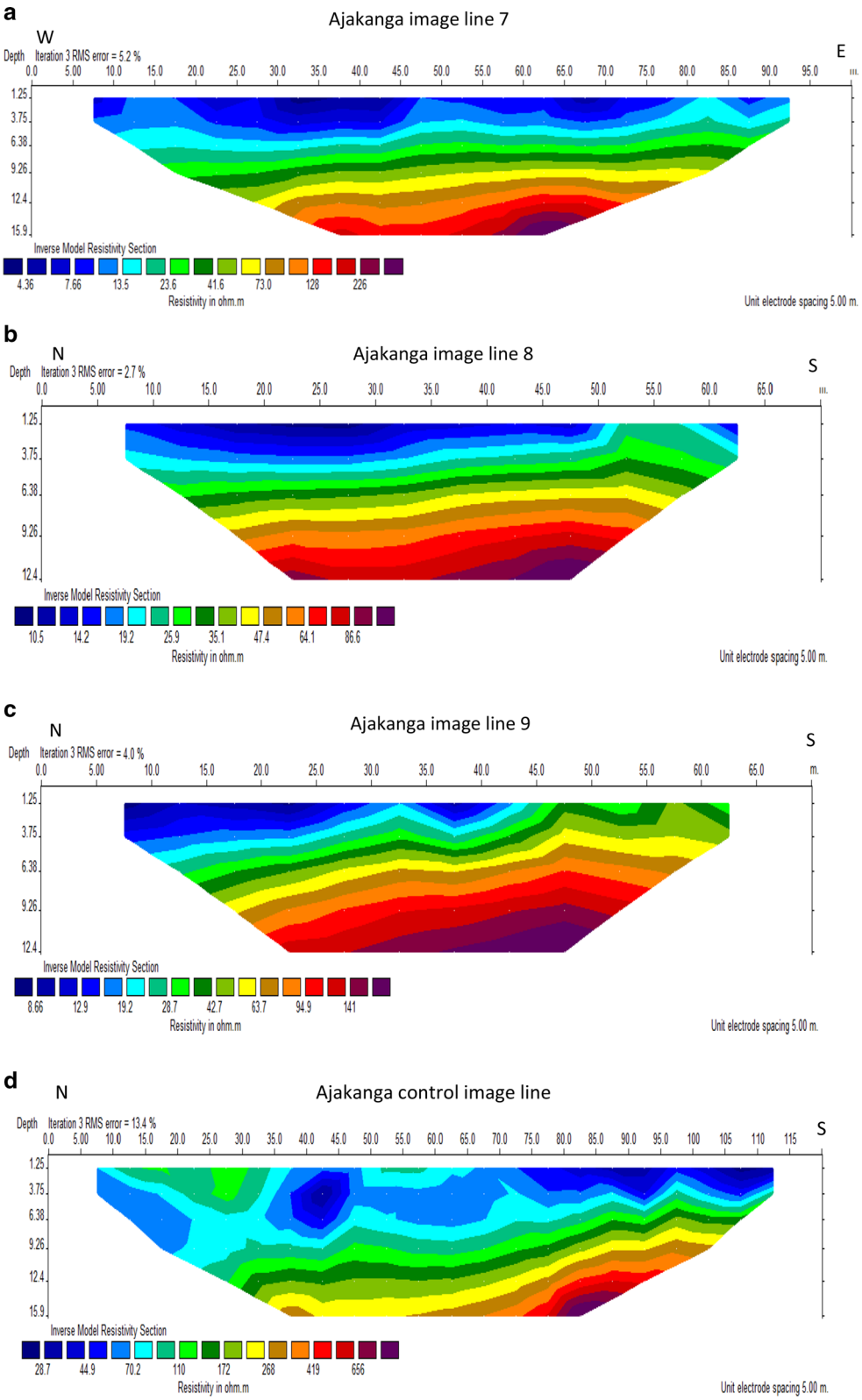

Fig. 9 2D inverse model resistivity sections for Ajakanga traverses 7, 8, 9 and control

20 Ω m. Weathered basement rock with resistivity values between 70 and 268 Ω m were noticed at depth while the measurement encounters the bedrock at position 75–95 m in the southern end of the traverse at depth greater than 12 m with resistivity values between 419 and 656 Ω m.

Interpretation of 3D inverse model resistivity images

Horizontal section of Ajakanga dumpsite

After applying the inversion process to the collated 2D data profiles with the aid of RES3DINV, six horizontal sections were obtained. The sections were modeled by RES3DINV as horizontal sections after five iterations with RMS error of 8.59 %. These sections covered from the surface to a depth of 21.9 m. The resistivity values range from a minimum of 4 Ω m to a maximum of 259 Ω m. The first four horizontal layers from the surface to a depth of 12.5 m showed complex subsurface which are more heterogenous when compared to layers 5 and 6 (Fig. 10). The heterogeneous nature of the first four layers could be due to the effect of leachate accumulation, clay soil, non degradable solid waste or exposure of dry soil due to removal and clearing of solid waste to create more space for dumping of solid waste materials. The resistivity ranged between 13 and 259 Ω m in layers 5 and 6 at 12.5–21.9 m depth with no traces of any low resistive region indicating that layers 5 and 6 contain weathered/fractured basement and fresh basement. Layers 5 and 6 showed a pronounced spread of basement region with resistivity values ranging from 142 Ω m to more than 259 Ω m as depicted in Fig. 10.

Vertical section of Ajakanga dumpsite

The vertical sections show the resistivity distribution in the *X*–*Z* plane for the layers to a depth of 19.4 m. The vertical sections as obtained by inversion process using RES3DINV showed 45 XZ plane where *X* is the profile direction and *Z* is the depth as shown in Figs. 11 and 12. There is combination of low and high resistivities zones in the first plane. This low resistive region could be interpreted as leachate plume observed from the traverses. Plane 2–20 for $Y = 21$–116 m contains resistivity values

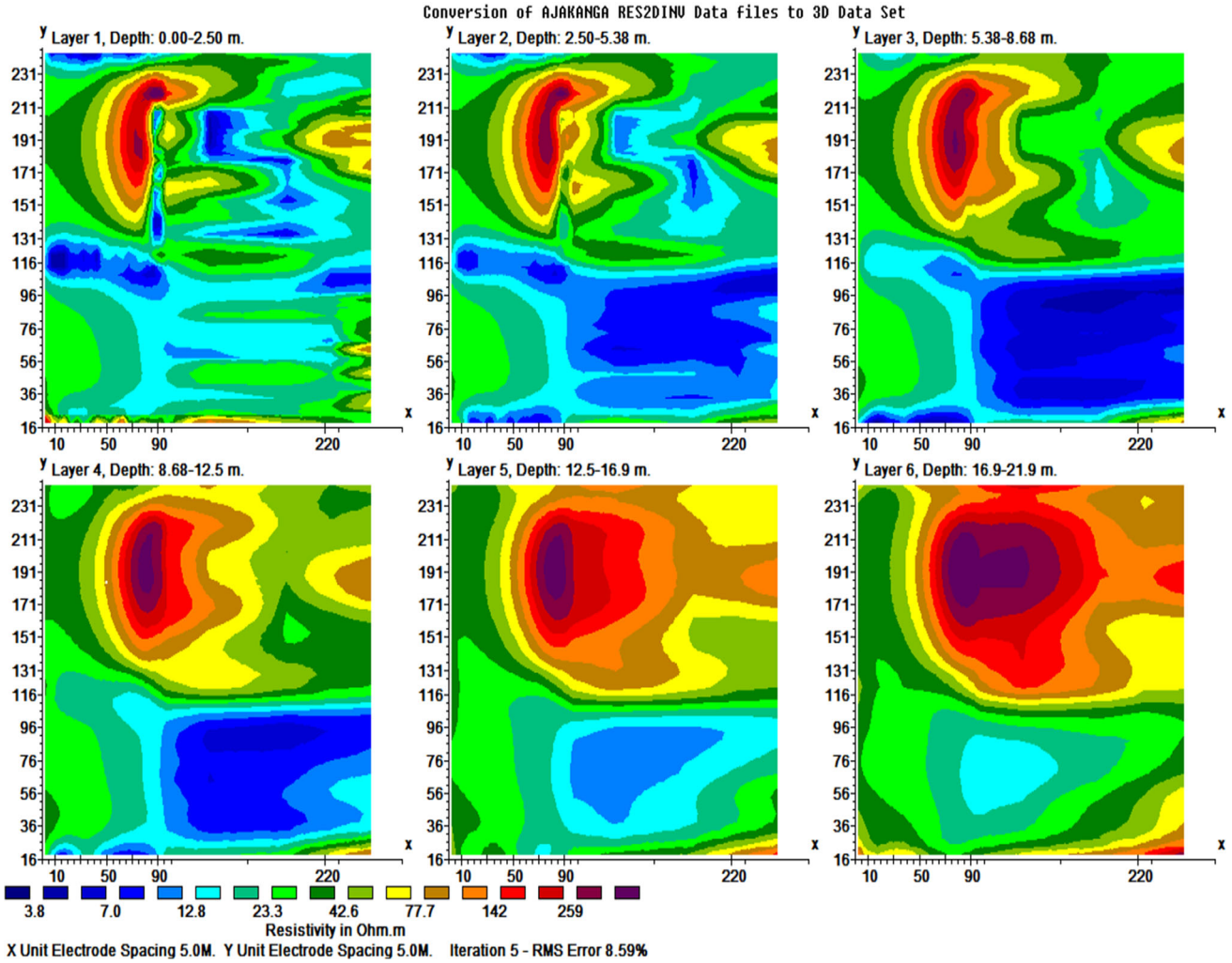

Fig. 10 Horizontal depth slices obtained from the 3D inversion of orthogonal 2D profiles on Ajakanga dumpsite

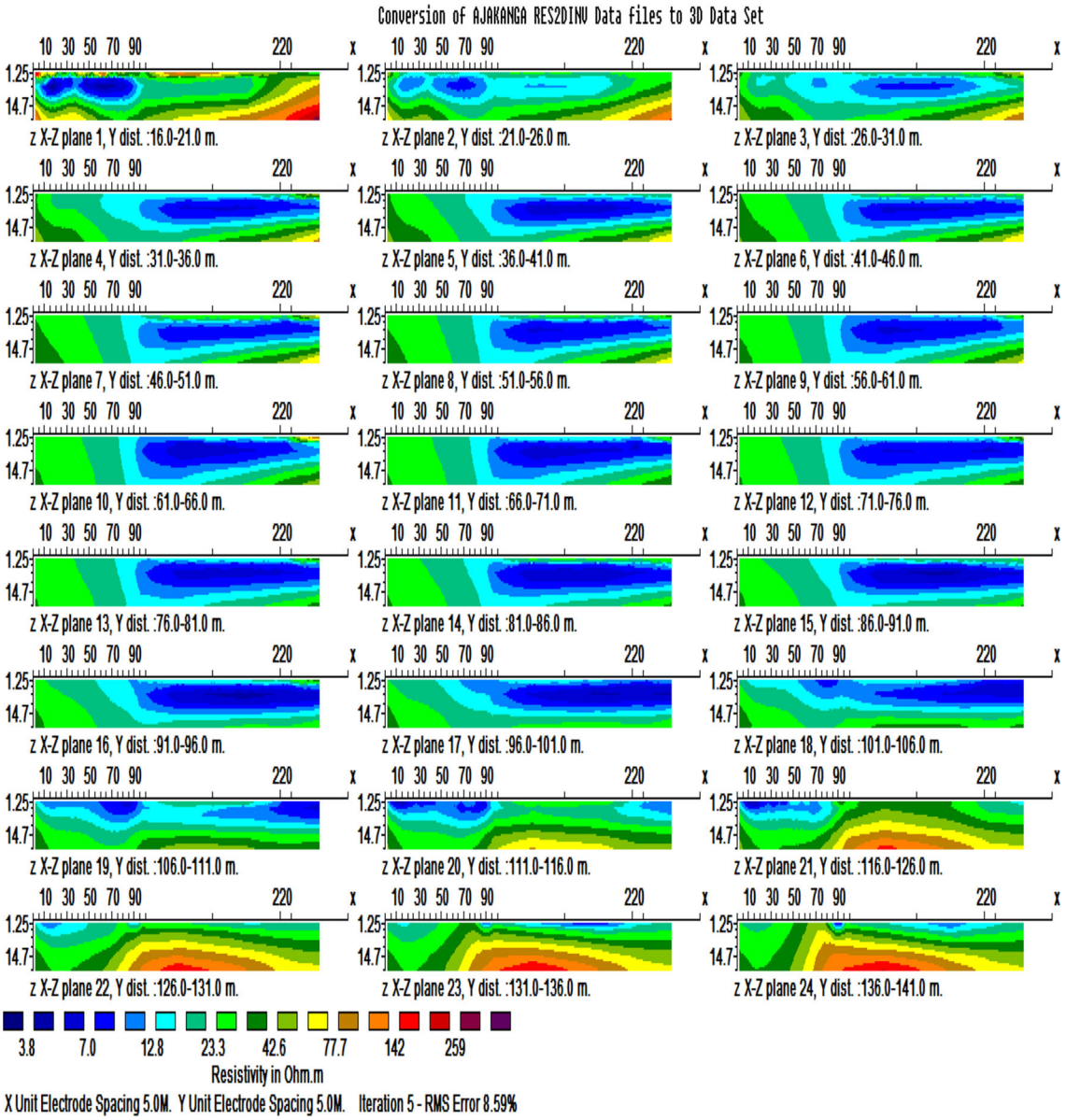

Fig. 11 Extracted 2D images in *X–Z* plane from the 3D constrained inverse resistivity model at the location of 2D profile measured on Ajakanga dumpsite

between 7 and 78 Ω m showing weathered basement while from plane 21–45 show resistivity value ranging from 7 to 259 Ω m suggesting fracture and basement rock units. The resistivity values for vertical sections at Ajakanga dumpsite ranges from 4 to 259 Ω m.

Groundwater quality for drinking purpose

Table 1 shows distance of the hand-dug wells to the landfill, depth of the well as well as depth to static water level for both seasons. Maximum and minimum concentrations of major ions present in the water samples and their percentage compliance with WHO and NSDWQ limits for both dry and wet seasons are as shown in Table 2, while Table 3 shows the comparison between values of each parameter during dry and wet seasons sampling periods.

The pH values of groundwater samples during dry and wet seasons sampling periods ranged from 6.9 to 7.8 and 6.7 to 7.3 respectively. The pH values for the two seasons lie within the permissible limit. The total dissolved solids (TDS) concentrations during March and August, 2013 varied from 88 to 299 mg/L and 95 to 351 mg/L respectively. All TDS values lie below 500 mg/L specified by WHO (2007) and NSDWQ (2007) limits. Electrical conductivity values ranged from 176 to 598 µS/cm in dry season and from 191 to 705 µS/cm in wet season. EC

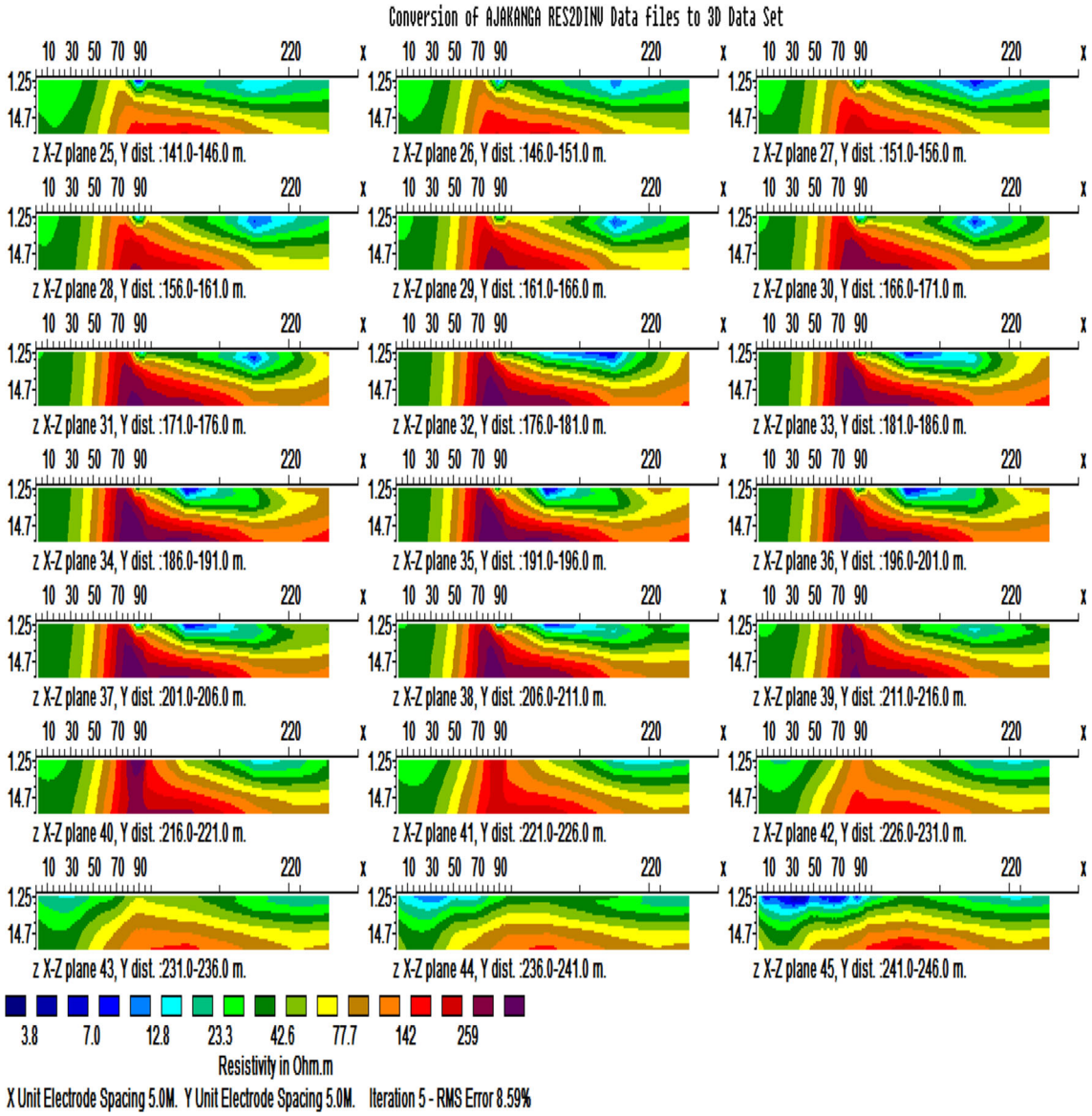

Fig. 12 Extracted 2D images in *X–Z* plane from the 3D constrained inverse resistivity model at the location of 2D profile measured on Ajakanga dumpsite

values in both season lie within the standard limit of WHO and NSDWQ (1000 µS/cm). The TDS values in both seasons showed all the groundwater samples to be of freshwater origin. The average concentration of total hardness (TH) varies from 46 to 406 mg/L and 116 to 432 mg/L during dry and wet seasons respectively. Based on Sawyer and McCarthy (1967) classification for TH, 20 % fall under "soft class", 40 % under "Hard class", 30 % under "moderate" class while the remaining 10 % falls under "very hard" class during dry season. However, during the wet season, none of the samples falls under "soft" class of hardness, 10 % falls under "moderate" class, 60 % fall under "Hard" class while 30 % fall under "Very Hard" Class. At all sampling locations, TH values were higher in wet season and lower in dry season. The chloride concentration of water samples during dry and wet seasons ranged from 16 to 113 mg/L and 10 to 53 mg/L, respectively. The observed values of chloride ions in both seasons were within the permissible limit of 250 mg/L.

Nitrate concentration in groundwater ranged from 1.5 to 15.9 mg/L during dry season and 0 to 3.9 mg/L during wet season. The nitrate values for both seasons were found to be within the limit of 50 mg/L specified by WHO (2007). The values of sulphate ions in the groundwater samples ranged from 14.4 to 127.7 mg/L and 7.6 to 52.3 mg/L during dry and wet seasons respectively. However,

Table 1 Well parameter for Ajakanga water samples (Dry and Wet seasons)

Well	Distance to landfill	Depth to water table (m) (dry)	Depth to water table (m) (wet)	Depth to bottom
1	90	3.7	2.7	9.1
2	110	2.0	2.1	2.7
3	100	3.5	3.2	3.5
4	200	5.8	2.7	6.4
5	220	5.2	2.7	5.5
6	200	4.6	4.3	5.5
7	270	5.5	3.2	5.8
8	520	7.2	6.5	8.2
9	120	–	–	–
10	120	1.8	1.8	3.7

Table 2 Comparison of groundwater quality parameters of Ajakanga with WHO (2007)/NSDWQ (2007) specification limits (dry and wet season)

Parameters	Dry		Percent compliance (dry)	Wet		Percent compliance (wet)	WHO and NSDWQ
	Min	Max		Min	Max		
pH	6.97	7.81	100	6.71	7.33	100	6.5–8.5
EC	176	598	100	191	705	100	1000
TDS	88	299	100	95	351	100	500
Cl^-	16	113	100	10	53	100	250
HCO_3^-	122	586	100	122	610	100	1000
CO_3^{2-}	60	288	40	60	300	50	120
TH	46	406	50	116	432	10	150
Na^+	12	30	100	11	24	100	200
K^+	1.00	6.00	100	1.00	6.00	100	55
NO_3^-	1.54	15.9	100	.00	3.90	100	50
Ca^{2+}	1.32	49.2	100	2.01	173.4	100	75
Mg^{2+}	1.12	14.23	100	3.29	49.34	100	50
SO_4^2	14.36	127.74	100	7,58	52.26	100	250

sulphate values in both seasons lie below 250 mg/L according to WHO (2007) and NSDWQ (2007) limit. Carbonate values in dry and wet seasons ranged from 60 to 288 mg/L and 60 to 300 mg/L; and bicarbonate values ranged from 122 to 586 mg/L and 122 to 610 mg/L in dry and wet seasons respectively.

The Ca^{2+} and Mg^{2+} concentration values during both seasons ranged from 1.3 to 49.2 mg/L and 2.0 to 173.4 mg/L; 1.1–14.2 mg/L and 3.3–49.3 mg/L respectively. Na^+ concentration value in groundwater ranged from 12 to 30 mg/L and 11 to 24 mg/L during dry and wet seasons, respectively. There is no significant seasonal variations of K^+. The lowest and highest concentration of K^+ in groundwater may be due to the fact that most potassium bearing minerals are resistant to decomposition by weathering processes and fixation in the formation of clay minerals (Scheytt 1997).

The degree of a linear association between any two of the analyzed parameters measured by Pearson's correlation coefficients for both seasons are presented in Tables 4 and 5 respectively. There is a very strong associations between EC and TDS, HCO_3^- and CO_3^{2-} during both seasons. Highly significant correlation between EC and TDS buttresses the fact that EC depends largely on the quality of the dissolved salts present in the sample. There is a negative correlation between Na^+ and K^+, TH and NO_3^- during both seasons. The negative correlation between TH and NO_3^- and between Na^+ and K^+ were expected because the effect of nitrogen fixing bacteria decreases with increasing hardness of water (Fabiyi 2008) while K^+ ion is normally less than

Table 3 Physico-chemical parameters during dry and wet seasons for Ajakanga water samples

Sample	pH		EC		TDS		Cl^-		HCO_3^-		CO_3^-		TH		Na^+		K^+		SO_4^{2-}		NO_3^-		Mg^{2+}		Ca^{2+}	
	Dry	Wet	Dry	Wet	Dry	Wet	Dry	Wet	Dry	Wet	Dry	Wet	Dry	Wet	Dry	Wet	Dry	Wet	Dry	Wet	Dry	Wet	Dry	Wet	Dry	Wet
S_1	7.1	7.0	598	465	299	237	96	52	414.8	317.2	204	156	180	432	30	22	2	1	26.45	25.49	1.8	.1	13.88	18.02	24.01	20.76
S_2	7.1	7.3	420	425	210	214	24	33.5	195.2	366	96	180	276	404	17	18	5	3	14.36	16.45	2.2	0	13.61	23.32	18.26	22.63
S_3	7.4	6.9	367	377	184	185	24	13	292.8	414.8	144	204	178	350	13	17	1	1	19.68	7.58	1.5	0	12.69	20.07	8.12	14.27
S_4	7.8	7.3	275	259	138	128	54	10.5	585.6	268.4	288	132	100	234	16	17	4	6	38.71	15.32	2.7	0	10.35	5.89	5.38	23.05
S_5	7.4	7.1	176	205	88	101	16	10	219.6	219.6	108	108	46	180	18	11	2	1	57.74	18.23	10.2	2.9	1.12	3.29	.41	9.66
S_6	7.2	6.7	530	411	264	205	113	52.5	170.8	219.6	84	108	200	260	18	24	6	1	127.74	27.74	11.9	3.2	12.97	14.69	7.28	4.51
S_7	7.2	6.9	299	191	150	95	32	16.5	366	122	180	60	96	116	16	14	4	1	88.07	24.68	16.0	3.0	5.03	5.32	1.32	2.01
S_8	7.6	7.0	225	242	112	121	28	15	122	170.8	60	84	70	206	15	16	2	1	45.81	14.20	5.1	.9	5.68	5.42	2.19	8.43
S_9	7.3	7.2	273	251	137	125	26	13.5	268.4	219.6	132	108	118	210	12	15	3	2	21.77	14.20	5.8	3.9	11.63	9.64	9.02	10.88
S_{10}	6.9	7.2	568	705	284	351	39	40.5	536.8	610	264	300	406	190	19	24	2	2	29.19	52.26	3.4	2.6	14.23	49.34	49.18	173.42

The unit of Cations is in mg/L

NB All parameters are in unit of mg/L except pH (no unit) and EC in µS/cm

Na^+ in igneous rock, typical of basement complex formation (Scheytt 1997).

However, higher concentration of some parameters were noticed in Wells 1 and 10 which may be due to effect of leachate migration in the southern part of the dumpsite; nearness to dumpsite; agricultural run-off and fertilizer application. On the other hand, all investigated hand-dug wells revealed high concentration of coliform group of bacteria with no presence of *E. coli* during dry season in all analyzed samples (Table 6). However, there is presence of *E. coli* in water samples from wells 4 and 7 during wet season. The presence of *E. coli* in water indicates recent faecal contamination and may indicate possible presence of disease causing pathogens such as bacteria, viruses and parasites.

Hydrogeochemical facies of groundwater

Piper diagram (Piper 1944) has been traditionally and most commonly used to classify the water and waste-water into different water category based on the anion and cation concentrations in the form of major ion percentage. The relative abundance of cations $\left(Ca^{2+} \text{ and } Mg^{2+}\right)$ are first plotted on the cation triangle while relative abundance of anions $\left(Cl^-,\ SO_4^{2-} \text{ and } HCO_3 + CO_3^{2-}\right)$ are plotted on the anion triangle. The centrally placed quadrilateral field (diamond shaped) shows the overall chemical property of the water sample from which inferences can be drawn on the basis of hydrogeochemical concept. Hydrochemical concept can help to elucidate the mechanism of flow and transport in groundwater systems (Hem 1985). The Piper plot (Fig. 13) shows the hydrogeochemical facies during both dry and wet seasons. From the plot, during dry season, 30 % of points lie within $(Na^+ + K^+)$ axis, 10 % lies in (Mg^{2+}) axis, 10 % lies in (Ca^{2+}) axis while 50 % of points fall in "No dominant" axis. In anions region of the plot, almost all the points (90 % of the water samples) lie within $(HCO_3^- + CO_3^{2-})$ axis while only 10 % lie in "No dominant" axis. Alkaline earth $\left(Ca^{2+} \text{ and } Mg^{2+}\right)$ exceed the alkalis $(Na^+ + K^+)$ and weak acids type $(HCO_3^- + CO_3^{2-})$ exceed the strong acids $(SO_4^{2-} \text{ and } Cl^-)$. Further analysis of the piper plot shows that 10 % are of $NaHCO_3$ (alkali rich type), 20 % are of mixed type (mixed $CaNaHCO_3$), only 10 % are of CaMgCl while the remaining 60 % are of $CaHCO_3$ type (freshwater).

During wet season, majority of groundwater samples are still of $\left(Ca^{2+} + Mg^{2+}\right)$ type i.e., alkaline earth exceeds the alkalis $(Na^+ + K^+)$. This is an indication that there is no change of this type irrespective of the season and hence the source of these ions

Table 4 Correlation coefficient of Ajakanga water samples parameters during dry season

	EC	TDS	Cl	Bicarbonate	Hardness	Carbonate	SO_4	NO_3	Na	K	Mg	Ca
EC	1											
TDS	1.000[b]	1										
Cl	.680[a]	.678[a]	1									
Bicarbonate	.282	.286	.121	1								
Hardness	.784[b]	.784[b]	.165	.308	1							
Carbonate	.282	.286	.121	1.000[b]	.308	1						
SO_4	.032	.029	.504	−.256	−.229	−.256	1					
NO_3	−.264	−.266	.078	−.271	−.381	−.271	.837[b]	1				
Na	.640[a]	.640[a]	.614	.270	.226	.270	−.004	−.162	1			
K	.154	.152	.422	−.153	.079	−.153	.569	.409	−.076	1		
Mg	.795[b]	.796[b]	.448	.289	.746[a]	.289	−.302	−.588	.230	.170	1	
Ca	.748[a]	.749[a]	.148	.490	.907[b]	.490	−.376	−.460	.421	−.185	.642[a]	1

[a] Correlation is significant at the .05 level (2-tailed)

[b] Correlation is significant at the .01 level (2-tailed)

Table 5 Correlation coefficient of Ajakanga water samples parameters during wet season

	EC	TDS	Cl	CO_3	HCO_3	Hardness	SO_4	NO_3	Na	K	Mg	Ca
EC	1											
TDS	1.000[b]	1										
Cl	.717[a]	.729[a]	1									
CO_3	.889[b]	.882[b]	.344	1								
HCO_3	.889[b]	.882[b]	.344	1.000[b]	1							
Hardness	.379	.391	.473	.338	.338	1						
SO_4	.738[a]	.738[a]	.595	.541	.541	−.235	1					
NO_3	−.130	−.135	−.020	−.253	−.253	−.704[a]	.360	1				
Na	.375	.387	.775[b]	.055	.055	.626	.069	−.296	1			
K	−.034	−.037	−.238	.131	.131	.036	−.104	−.367	−.020	1		
Mg	.961[b]	.957[b]	.538	.934[b]	.934[b]	.243	.730[a]	−.057	.155	−.022	1	
Ca	.816[b]	.809[b]	.311	.840[b]	.840[b]	−.129	.836[b]	.103	−.145	.114	.887[b]	1

[a] Correlation is significant at the .05 level (2-tailed)

[b] Correlation is significant at the .01 level (2-tailed)

$(Ca^{2+} + Mg^{2+})$ may be natural. In terms of weak acids/strong acids, all the groundwater samples in wet season are of weak acid type. When seasonal changes of the water type are considered, for the wet season of the cation region of the plot, only 10 % lies within $(Na^+ + K^+)$ axis; 10 % in the (Mg^{2+}) axis; 10 % in the (Ca^{2+}) axis while remaining 70 % fall in "No dominant type" region. In anions region of the plot, all the water samples lie within $(HCO_3^- + CO_3^-)$ axis while none fall within the "No dominant type" region.

Discussion: 2D and 3D ERT results

The 2D inverted sections in electric resistivity tomography showed the infiltration and migration of leachate plume from one point to another within the dumpsite. The electrical resistivity imaging has the advantage of obtaining two dimensional evolution of leachate plume (Paul et al. 2007). The 2D electrical imaging method reveals the inverse models of resistivity distribution of the subsurface and varying lithologies with depth. The migration of lea-

Table 6 Result of microbial analysis of water samples during dry and wet seasons

Sample code	Dry		Wet	
	Coliform count	*E. coli*	Coliform count	*E. coli*
S_1	1.14×10^4	0	4.6×10^3	0
S_2	9.2×10^3	0	1.2×10^4	0
S_3	5.2×10^3	0	3.0×10^3	0
S_4	2.2×10^3	0	1.34×10^4	6
S_5	1.24×10^4	0	5.8×10^3	0
S_6	1.42×10^4	0	1.4×10^3	0
S_7	1.68×10^4	0	1.56×10^4	2
S_8	7.6×10^3	0	6.2×10^3	0
S_9	1.38×10^4	0	1.0×10^4	0
S_{10}	1.72×10^4	0	3.6×10^3	0

chate plume as observed from inverse models was traced in the form of low resistivity zones with resistivity values less than 20 Ω m. It should be noted that the inverse model of 3D inversion of Ajakanga indicate that the abnormally high resistivity value of the order of >1000 Ω m observed in 2D resistivity imaging has been eliminated. Furthermore, the effective depth of investigation as observed in 3D inversion models is greater than 15.9 m (precisely 21.9 m).

It was observed from the models of the resistivity traverses within Ajakanga dumpsite that, the traverses towards the southern part of the dumpsite showed clearer picture of leachate plume migration than those on the northern side of the dumpsite. This can be likened to the flow of leachate from decomposed wastes moving from the northern side of the dumpsite towards the southern part where it accumulates and it is of greater extent than one on the northern side.

Conclusion

The integrated approach of electrical imaging methods and hydrogeochemical investigation were employed to investigate groundwater contamination around Ajakanga dumpsite while Hydrogeochemical facies of groundwater samples from hand-dug wells were revealed through Piper diagram analysis. The integrated methods have led to a better understanding of the site than could have been achieved with the use of a single investigative method. The interpretation of 2D resistivity models of traverses within Ajakanga dumpsite showed low resistive zones with true resistivity values less than 20 Ω m as indicative of leachate plume and 15.9 m as maximum depth of investigation. The horizontal and vertical extent of leachate plumes were delineated by 2D geoelectrical imaging as a response of the varying electrical conductivity in the dumpsite. Profile ran on the southern part of the dumpsite show strong evidence of horizontal and vertical plume migration; an evidence that most of the decomposition process of leachate and its run off take place mostly in the southern part due to sloppy topography of this side. This is also buttressed by elevated concentrations of most physic-chemical parameters of groundwater from hand-dug well 1 which is located directly opposite the dumpsite and of about 90 m distance

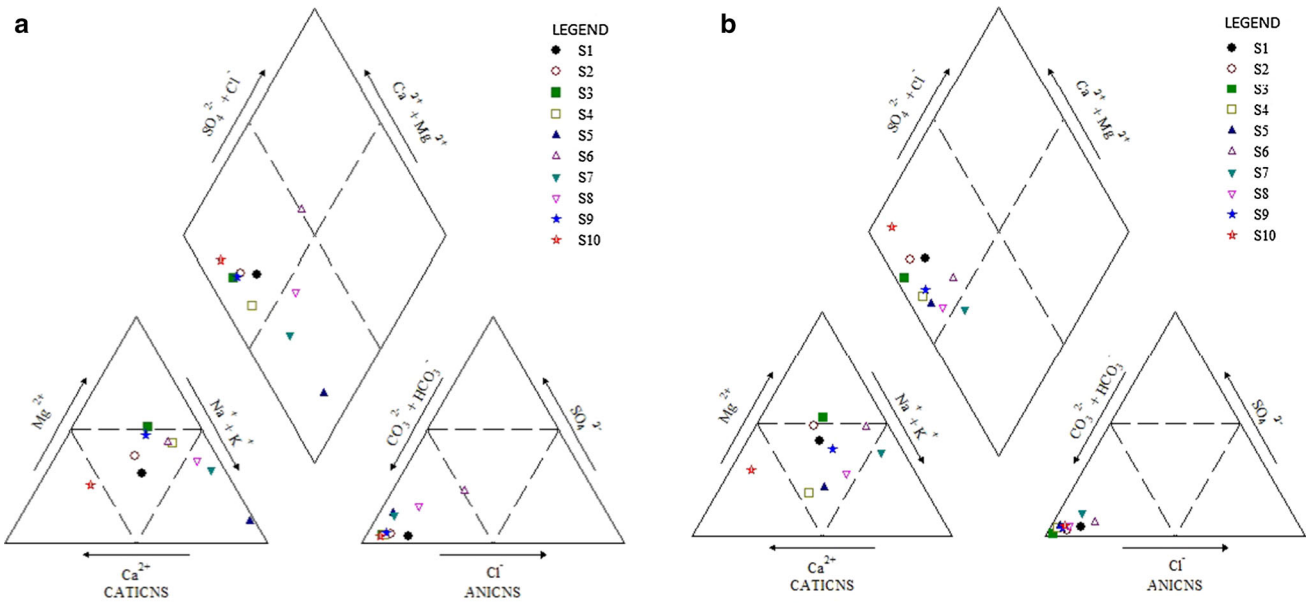

Fig. 13 Piper Trilinear diagram for Ajakanga water samples for **a** dry and **b** wet seasons

to the dumpsite. The result of physio-chemical parameters on analyzed groundwater samples lie within WHO (2007)/ NSDWQ (2007) specification limits for drinking purpose. However, effect of leachate migration, nearness to dumpsite, agricultural run-off and fertilizer application might have caused higher concentrations of some parameters in wells 1 and 10 respectively. There is possible contamination of shallow groundwater system in the southern part of the dumpsite as dumpsite ages due to strong evidence of leachate migration and extent of migration depth on this side of the dumpsite. With the help of Piper diagram, the interpretation of hydrochemical facies of groundwater samples in both dry and wet seasons show dominant water type to be of $CaHCO_3$. Generally, the groundwater quality of the study area in both seasons based on the interpretation of hydrochemical analysis is hard, fresh and alkaline in nature. Repeated resistivity method accompanied by chemical analyses of groundwater samples from nearby hand-dug wells bordering the dumpsite should be adopted for tracing the future position of leachate plume in space and time, and up to date status of hand-dug wells for drinking and consumption purposes as the dumpsite ages.

References

Journal article

Abdullahi NK, Osazuwa IB, Sule PO (2011) Application of integrated geophysical techniques in the investigation of groundwater contamination. A case study of municipal solid waste leachate. Ozean J Appl Sci 4(1):7–25

Adepelumi AA, Ako BD, Ajayi TR, Afolabi O, Omotoso EJ (2008) Delineation of Saltwater Intrusion into the freshwater Aquifer of lekki Penni sula, Lagos, Nigeria. Environ Geol 56(5):927–933

Afolayan OS, Ogundele FO, Odewunmi SG (2012) Hydrological implication of solid waste disposal on groundwater quality in urbanized area of Lagos state, Nigeria. Int J Appl Sci Tech 2(5):74–82

Andrea TU, Vagner RE, Giulliana M, Lazaro VZ, Heraldo LG (2012) Case study: a 3D resistivity and Induced polarization imaging from downstream in waste disposal site in Brazil. Environ Earth Sci 66:763–772

Ariyo SO, Enikanoselu EM (2007) Integrated use of geoelectrical Imaging and geochemical analysis in the environmental impact assessment of Egbe dumpsite in Ijebu-Igbo area, southwestern Nigeria. Cont J Earth Sci 1:11–17

Armah FA, Luginaah I, Ason B (2012) Water quality index in the Takwa gold mining area in Ghana. J Transdiscipl Env Stud 11(2):1–15

Assmuth TW, Strandberg T (1993) Groundwater contamination at Finnish landfills. Water Air Soil Pollut 69:163–175

Atekwana EA, Sauck WA, Werkema DD Jr (2000) Investigations of geoelectrical signatures at a hydrocarbon contaminated site. J Appl Geophys 44:167–180

Ayolabi EA, Folorunso AF, Eleyinmi AF, Anuayah EO (2009) Application of 1D and 2D electrical resistivity methods to map aquifers in a complex geologic terrain of foursquare camp, Ajebo, southwestern Nigeria. Pac J Sci Technol 10(2):657–666

Badejo AA, Taiwo AO, Bada BS, Adekunle AA (2013) Groundwater quality assessment around municipal solid waste dumpsite in Abeokuta, southwestern, Nigeria. Pac J Sci Tech 14(1):593–603

Bagarello V, Sgroi A (2007) Using the simplified falling head technique to detect temporal changes in field-saturated hydraulic conductivity at the surface of a sandy loam soil. Soil Tillage Res 94:283–294

Bayowa OG, Olayiwola NS (2015) Electrical resistivity investigation for topsoil thickness, competence and corrosivity evaluation: a case study from Ladoke Akintola University of Technology, Ogbomoso, Nigeria. 2nd international conference on geological and civil engineering. IPCBEE/ACSIT Press, Singapore, 80, pp 52–56

Elueze AA (2000) Compositional appraisal and petrotectonic significance of the Imelu banded ferraginous rock in Ilesha Schist Belt, South western, Nigeria. J Min Geol 36(1):9–18

Fabiyi IP (2008) Depth of hand-dug wells and water chemistry. Example from IBNE Local Government Area, Oyo state, Nigeria. J Soc Sci 17(3):261–266

Fortier R, Allard M, Seguin MK (1994) Effects of physical properties of frozen ground on electrical resistivity logging. Cold Reg Sci Technol 22:361–384

Ikem A, Osibanjo O, Sridliar MKC, Sobande A (2002) Evaluation of groundwater quality characteristics near two waste sites in Ibadan and Lagos, Nigeria. Water Air Solid Pollut 140:307–333

Iyoha AA, Amadasun CVO, Evboumwan IA (2013) 2D Resistivity Imaging investigation of solid waste landfill sites in Ikhyeniro municipacity. Ikpoba Okha Local Government Area, Edo State, Nigeria. J Resour Dev Manag 1:65–69

Jegede SI, Osazuwa IB, Ujuanbi O, Chiemeke CC (2011) 2D electrical imaging survey for situation assessment of leachate plume migration at two waste disposal sites in the Zaria basement complex. Adv Appl Sci Res 2(6):1–8

Johansson S, Rosqvist H, Svensson M, Dahlin T, Leroux V (2011) An alternative methodology for the analysis of electrical resistivity data from a soil gas study. Geophys J Int. doi:10.1111/j.1365-246x.2011.05080.x

Karlik G, Kaya MA (2001) Investigation of groundwater contamination using electric and electromagnetic methods at an open waste-disposal site. A case study from Isparta, Turkey. Environ Geol 40(6):725–731

Kasprzak M (2015) High-resolution electrical resistivity tomography applied to patterned ground, Wedel Jarlsberg land, south–west Spitsbergen. Polar Res 34:25678. doi:10.3402/polar.v34.25678

Kayabali K, Yuksel FA, Yeken T (1998) Integrated use of hydrochemistry and resistivity methods in groundwater contamination caused by a recently closed solid waste site. Environ Geol 36(3–4):227–234

Kneisel C, Hauck C, Fortier R, Moorman B (2008) Advances in geophysical methods for permafrost investigations. Permafrost Periglac Process 19(2):157–178

Kumar D (2012) Efficacy of ERT technique in mapping shallow subsurface anomaly. J Geol Soc India 80:304–307

Lateef TA (2012) Geophysical investigation of groundwater using electrical resistivity method—a case study of Annunciation Grammar School, Ikere lga, Ekiti state, southwestern Nigeria. IOSR J Appl Phys 2(1):01–06

Loke MH, Barker RD (1996) Rapid least squares inversion of apparent resistivity pseudosections by a quasi-Newton method. Geophys Prospect 44:131–152

Matias MS, Marques da Silva M, Ferreira P, Ramalho E (1994) A geophysical and hydrogeological study of aquifers contamination by a landfill. J Appl Geophys 32:155–162

Mazac O, Kelly WE, Landa I (1987) Surface geoelectics for groundwater pollution and protection studies. J Hydrol 93:277–294

Metwaly M, Khalil MA, Al-Sayed ES, El-Kenawy A (2012) Tracing subsurface oil pollution leakage using 2D electrical resistivity tomography. Arab J Geosci. doi:10.1007/S12517-012-0600-z

Mondelli G, Giacheti HL, Howie JA (2010) Interpretation of Resistivity piezocone tests in a contaminated municipal solid waste disposal site. Geotech Test J 33(2):1–14

Munoz-Castelblanco JA, Pereira JM, Delage P, Cui YJ (2011) The influence of changes in water content on the electrical resistivity of a natural unsaturated Loess. Geotech Test J 35(1):1–7

Oladunjoye MA, Olayinka AI, Amidu SA (2011) Geoelectrical imaging at an Abandoned waste dumpsite in Ibadan, southwestern, Nigeria. J Appl Sci 11(22):3755–3764

Paul TI, Debra RR, Marja E, Roger G, Nitin GBH, Sreeram J, Timothy GT, Ramin Y (2007) Review of state of the art methods for measuring water in landfills. Waste Manag 27:729–745

Piper AM (1944) A graphical procedure in the geochemical interpretation of water analysis. Trans Am Geophys Union 25:914–923

Ramakrishnaiah CR, Sadashivaiah C, Ranganna G (2009) Assessment of water quality index for groundwater in Tunikur Taluk, Kamataka state, India. E J Chem 6(2):523–530

Rizwan R, Gurdeep S (2010) Assessment of groundwater quality status by using water quality index method in Orissa, India. World Appl Sci J 9(12):1392–1397

Sasaki Y (1992) Resolution of resistivity tomography inferred from numerical simulation. Geophys Prospect 40:453–464

Scheytt T (1997) Seasonal variations in groundwater chemistry near Lake Belau, Schleswig—Holstein, Northern Germany. Hydrogeol J 5(2):86–95

Soupios P, Papadopoulos I, Kouli M, Georgaki I, Vallianatos F, Kokkinous E (2006) Investigation of waste disposal areas using electrical methods: a case study from Chania, Crete, Greece. Environ Geol. doi:10.1007/S00254-006-0418-7

Tijani MN, Onibalusi SO, Olatunji AS (2002) Hydrochemical and environmental impact assessment of Orita Aperin waste dumpsite, Ibadan, southwestern, Nigeria. Water Resour 13:78–84

Ustra AT, Elis VR, Mondelli G, Zuquette LV, Giacheti HL (2012) Case study: a 3D resistivity and induced polarization imaging from downstream a waste disposal site in Brazil. Environ Earth Sci 66:763–772

Win Z, Hamzah U, Ismail MA, Samsudin AR (2011) Geophysical investigation using resistivity and GPR: a case study of oil spill site at Seberang, Prai, Penang. Bull Geol Soc Malays 57:19–25. doi:10.7186/bgsm001

Yalo N, Lawson M, Adihou C (2014) Geophysical contribution for the mapping of the contaminant plume of leachate from Rubbish Dumpsite of Herie, Benin. Br J Appl Sci Tech 4(1):127–143

Yamasaki MT, Peixoto AS, Lodi PC (2013) Evaluation of electrical resistivity in a tropical sandy soil compacted. Electron J Geotech Eng(EJGE) 19:629–644

Book

Akintola JO (1986) Rainfall distribution in Nigeria, 1892–1983. Impact publishers, Ibadan **380 pp**

Dane JH, Hopmans JW (2002) Water retention and storage. In: Dane JH, Topps GC (eds) Methods of soil analysis part 4; physical methods. Soil Science Society of America, Madison, pp 671–690

Gulser C, Candemir F (2008) Prediction of saturated hydraulic conductivity using moisture constants and soil physical properties **Samsun 55139**

Jones HA, Hockey RD (1964) The geology of southwestern Nigeria. Geological survey of Nigeria Ball 31 **89 pp**

Kirkham MB (2005) Principles of soil and plant water relations. Elsevier Academic Press, Burlington, pp 145–172

Sawyer GN, McCarthy DL (1967) Chemistry of sanitary engineers, 2nd edn. McGraw Hill, New York **518 p**

Yu QH, Cheng GD, Wang WL (2003) The progress of permafrost investigation with geophysical methods in China. In: Permafrost, Phillips, Springman and Arenson (eds), Swets and Zeitlinger, Lisse, ISBN 90 5809 5827. pp 1271–1276

Online document

APHA (2005) Standard methods for the examination of water and waste water, 21st edn. American Public Health Association, Washington

Benson R, Glaccum R, Noel M (1983) Geophysical techniques for sensing buried waste and waste migration. Environ monitor syst lab off Res Develop. Us Environ Protect Ag, Las Vegas, NV, Rep 68-03-3050

CPE (2010) Land recovery and use in Nigeria (Pre-feasibility studies using LFGE). Final report prepared for US Environmental Protection Agency by Centre for People and Environment **57 pp**

FAO (2015) IUSS working group WRB 2015. World reference base for soil resources 2014, update, 2015. International soil classification system for naming soils and creating legends for soil maps. World soil resources reports, No 106, FAO Rome **203 pp**

Hem JD (1985) Study and interpretation of the chemical characteristics of natural water. USGS water supply paper, vol 2254. pp 117–120

Loke MH (2000) RES2DINV version 3.44 for windows 95/98 and NT: rapid 2D resistivity and IP inversion using the least squares method. Advanced Geosciences Inc., Austin

NSDWQ (2007) Nigerian standard for drinking water quality. Nigeria Industrial Standard, NIS 554. Standard Organization of Nigeria, Lagos **30 pp**

WHO (2007) Water for pharmaceutical use in quality assurance of pharmaceuticals A compendium of Guidelines and Related materials, 2nd edn. World Health Organization, Geneva, pp 170–187